ACS Photonics

Article

pubs.acs.org/journal/apchd5

# Real-Time Observation of Ultrafast Intraband Relaxation and Exciton Multiplication in PbS Quantum Dots

Ala'a O. El-Ballouli,[†] Erkki Alarousu,[†] Anwar Usman, Jun Pan, Osman M. Bakr,* and Omar F. Mohammed*

Solar and Photovoltaics Engineering Research Center, Division of Physical Sciences and Engineering, King Abdullah University of Science and Technology, Thuwal 23955-6900, Kingdom of Saudi Arabia

Supporting Information

**ABSTRACT:** We examine ultrafast intraconduction band relaxation and multiple-exciton generation (MEG) in PbS quantum dots (QDs) using transient absorption spectroscopy with 120 fs temporal resolution. The intraconduction band relaxation can be directly and excellently resolved spectrally and temporally by applying broadband pump−probe spectroscopy to excite and detect the wavelengths around the exciton absorption peak, which is located in the near-infrared region. The time-resolved data unambiguously demonstrate that the intraband relaxation time progressively increases as the pump-photon energy increases. Moreover, the relaxation time becomes much shorter as the size of the QDs decreases, indicating the crucial role of spatial confinement in the intraband relaxation process. Additionally, our results reveal the systematic scaling of the intraband relaxation time with both excess energy above the effective energy band gap and QD size. We also assess MEG in different sizes of the QDs. Under the condition of high-energy photon excitation, which is well above the MEG energy threshold, ultrafast bleach recovery due to the nonradiative Auger recombination of the multiple electron−hole pairs provides conclusive experimental evidence for the presence of MEG. For instance, we achieved quantum efficiencies of 159, 129 and 106% per single-absorbed photon at pump photoexcition of three times the band gap for QDs with band gaps of 880 nm (1.41 eV), 1000 nm (1.24 eV) and 1210 nm (1.0 eV), respectively. These findings demonstrate clearly that the efficiency of transferring excess photon energy to carrier multiplication is significantly increased in smaller QDs compared with larger ones. Finally, we discuss the Auger recombination dynamics of the multiple electron−hole pairs as a function of QD size.

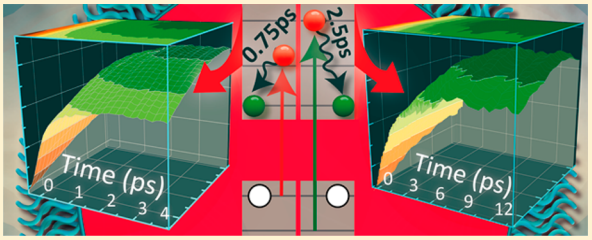


**KEYWORDS:** *intraconduction band relaxation, exciton multiplication, PbS quantum dots, femtosecond broadband transient absorption spectroscopy*

Multiple-exciton generation (MEG) for single high-energy photon absorption is one of the most remarkable features of semiconductor quantum dots (QDs) and other nanoscale materials.[1−5] It represents a possible new path toward increasing the conversion efficiency of solar cell devices.[6−8] These possibilities have encouraged researchers to study MEG extensively in a variety of QDs of different sizes, not only to understand the physics of this high-order phenomenon, but also to improve the conversion efficiency of solar cell devices through optimal-photon energy utilization.[2,9−12] In the MEG process, the excess energy of an absorbed high-energy photon is used to generate an electron or hole with kinetic energy greater than the lowest unoccupied molecular orbital−highest occupied molecular orbital (LUMO−HOMO) transition energy, that is, the energy band gap, $E_g$, of the semiconductor. This excess energy is transferred via the Coulomb interaction to the valence-band electron, exciting it across the energy band gap, to create one or more additional electron−hole pairs rather than being wasted as heat through electron−phonon interactions.[13] Theoretically, the high efficiency of the MEG process is attributed to the formation of a coherent superposition of single- and multiple-exciton states; the latter are generated extremely fast upon absorption of high-energy photons.[14,15] It was also found that the two types of states exhibit different decay rates and that the ratio of these rates determines whether a single photon can create a single exciton or multiple excitons.[16] On the other hand, there is mounting evidence that MEG in QDs may occur via a process of impact ionization, which is similar to the one operative in the bulk.[17] Due to quantum confinement, impact ionization in QDs is modified and the MEG efficiency in QDs is thus different from that of the bulk.

Several groups initially presented evidence of pronounced MEG manifestation in a variety of semiconductor QDs,[18−21] and a MEG quantum yield (QY) of seven excitons per single-absorbed photon (700%) was reported in PbSe QDs.[22] In sharp contrast, other experimental investigations have recently reported much lower yields or even the absence of MEG.[23−26] For instance, Nair et al.[24] reported that at most 0.25 additional electron−hole pairs were generated per single photon absorption in PbSe and PbS QDs, even under excitation

**Received:** January 17, 2014
**Published:** February 18, 2014

  

at photon energies five times their $E_g$. The contradicting assessments have raised serious concerns about the efficiency of MEG in QDs and warrant additional efforts not only to reassess MEG, but also to understand the electronic states involved in the excited QDs.

Electronic state-to-state relaxation is one of the most fundamental issues of concern in the photophysics of nanoscale materials. Due to large energy-level spacing in QDs, their carrier dynamics and electronic relaxation are significantly different from those in bulk materials.[9,27,28] Moreover, the existence of well-separated energy levels may act to reduce the rate of phonon emission from the highly excited carriers, and it may subsequently contribute to the efficient MEG.[29] In this regard, a profound understanding of the state-to-state transition involved in excited QDs, by which excitons with high kinetic energy can relax from higher to lower levels, is essential for utilizing QDs with optical gain[30] and MEG[2,18] in many potential applications.

From a practical perspective, ultrafast exciton dynamics, particularly the electronic structural dynamics in CdSe QDs, have been intensively explored using femtosecond-transient absorption and photoluminescence methodologies.[1,10,31−41] By applying pump−probe spectroscopy, QDs used in solar energy applications have been intensively investigated through experimental mapping of their intraband relaxation and exciton-multiplication dynamics.[1,2,41−43] While the fabrication of QDs has seen much progress,[44−48] the debate on fundamental dynamical information related to their electronic states remains open.[10,40,42,43] Specifically, the intraconduction band relaxation processes in PbS QDs have yet to be elucidated due in part to the limitations of current experimental techniques in pumping and detecting with broadband capabilities in the near-IR spectral region, where the first exciton absorption peak is located.[42] Significantly, the lack of such information hampers the accurate determination of whether the depopulation of high quantized states is due to carrier trapping at surface defects or to intraband relaxation into intrinsic QDs states.

Here, we report the real-time observation of intraband relaxation of PbS QDs as a function of pump-photon energy and QD size. By monitoring the ground state bleach and excited state absorption bands using femtosecond broadband transient absorption spectroscopy, we decipher and evaluate the intraband relaxation from higher excited states to the band edge ($1S_e$ state) of the QDs. More importantly, we provide conclusive experimental evidence of a strong size dependence of the quantum yield (QY) of MEG; MEG exists in small QDs $\leq$ 1210 nm in size, but it is absent in larger sizes under the same excitation conditions (three times the $E_g$). This observation verifies that the efficiency of transferring excess photon energy to the carrier multiplication is increased as the QD size decreases, leading to a reduced MEG threshold and an increased QY.

## RESULTS AND DISCUSSION

PbS QDs absorb light in the near-IR region, as representatively shown by the steady-state absorption spectra of two different sizes of PbS QDs (Figure 1). We assigned the well-defined absorption peaks centered at 1080 and 1355 nm to their $E_g$, equivalent to the lowest optical transition between spatially confined electron and hole states. The QDs are nearly spherical in shape, as indicated by TEM images in the top panels of Figure 1.

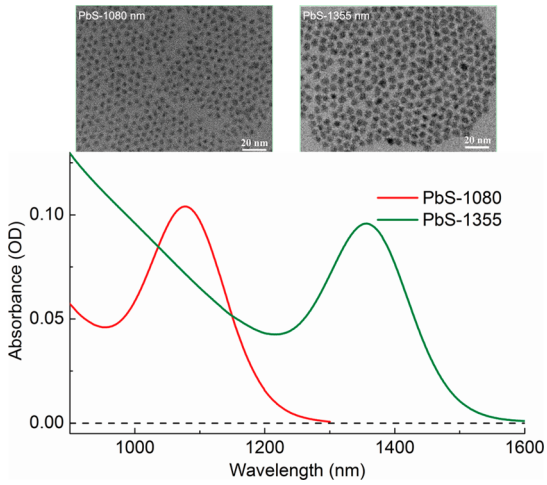


**Figure 1.** Steady-state absorption spectra of PbS-1080 (red) and PbS-1355 (green) in toluene, corresponding to $E_g$ of 1.15 and 0.92 eV, respectively. The top panel represents their HRTEM images with 20 nm scale bars. The well-defined absorption peak corresponds to the first exciton absorption peak (the $1S_h-1S_e$ transition).

Since the bleach recovery of the lowest absorption peak reflects the depopulation of excited carriers in the 1S state, we used it as a convenient probe to follow the electronic relaxation, carrier recombination, and multiplication dynamics of various sizes of PbS QDs with band gaps ranging from 0.79 eV (PbS-1560) to 1.41 eV (PbS-880). In Figure 2, we show the transient absorption (TA) spectra of PbS-1355 at different excitation

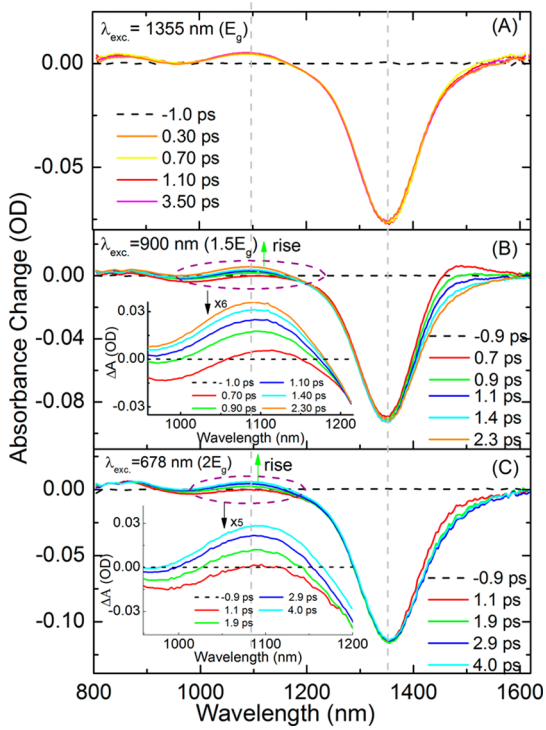


**Figure 2.** Averaged near-IR transient absorption spectra at indicated delay time windows after excitation at 1355 (A), 900 (B), and 678 nm (C). The $1S_e$ exciton bleach at 1355 nm is attributed to the state filling of the 1S electron and hole level, and the positive band at 1090 nm is caused by ESA. For clarity, the insets in (B) and (C) show magnified views of the formation of the ESA band.


dx.doi.org/10.1021/ph500016t | ACS Photonics 2014, 1, 285−292

wavelengths, 1355 (A), 900 (B), and 678 nm (C), corresponding to 1, 1.5, and 2 times the $E_g$, respectively. In addition to the ground state bleach at 1355 nm, due to the removal of the population from the occupied valence band, positive absorption bands appear at 1090 and 1480 nm. The photoinduced absorption features and assignments have been reported by Klimov et al.[49] Based on the spectral shape, the formation with zero excess energy (excitation in the band gap) and decay time constants at the different energies of photon excitation, the positive peak at 1090 nm is the exited-state absorption (ESA) of the excited charge carrier, while the positive peak at 1480 nm is a clear spectroscopic signature for hot electrons (see also Figure S2). This broad feature is observed when the band-edge states are unoccupied, that is, when the carriers are in the excited "hot" states, due to a Coulombic shift of the band-edge transition (usually referred to a biexciton shift).[37,39] After the carriers relax into the band-edge states, this feature becomes overwhelmed by the 1S bleaching. The dynamic responses of the ground state bleach and the band at 1090 nm after the intraband relaxation are very similar (Figure S3), supporting our assignment for the ESA. It is worth pointing out that the substantial spectral overlap with the ground state bleach at 950 and 1150 nm due to $1P_h \rightarrow 1P_e$ and $1S_h \rightarrow 1P_e$ transitions[29] makes the amplitude of the ESA band smaller compared with the ground state bleach at 1355 nm. We should also note that, because this peak does not show any spectral shift at different pumped-photon energies, we can therefore exclude the quantum-confined Stark effect that induces a red shift in the absorption spectrum.[50] Interestingly, the time constant of the formation of ESA band depends on the pump-photon energy. It instantaneously appears when the pump-photon energy is equal to the band gap energy (no excess electron kinetic energy), providing clear indication of an immediate population of the $1S_e$ state.

For the pump-photon energy at $E_g$, the electron is already loaded in the 1S state; hence, no further possible relaxation is expected and the nanosecond decay of this TA signal is due to electron repopulation via radiative recombination (Figure 2A). On the other hand, with the excess photon energy of the excitation pulse (Figure 2B,C), the formation of the ESA band shows a clear delay as it reaches its peak value within 2−8 ps. In this regime, the three-dimensional (3D) surface in Figure 3 presents the loading time of PbS-1355 electrons to the 1S state with pump pulses centered at wavelengths of 1.5, 2, and 2.8 times the $E_g$, demonstrating clearly the dependence of the electron loading time on the pumped-photon energy. The dynamical feature of the ESA band can be attributed to the intraband relaxation, that is, the loading of the exciton from higher-lying states into the electronically cold, band edge state. Simultaneously, the bleach recovery of the second electronic excited state centered at 950 nm, assigned as the $1P_h \rightarrow 1P_e$ transition,[51] is associated with ESA band formation (Figure 4). This finding provides strong experimental evidence of intraband relaxation from higher energy levels into the electronically cold 1S state.[42] Additionally, as a result of intraband relaxation, there is a rise in the magnitude of the 1S bleach, especially at early time delay (see also, Figure S2). However, the rise of the ground-state bleach is relatively small since we do suspect that some of the 1P electrons are going into trap-states at high energy levels, rather than relaxing into the 1S state, which is consistent with the picture of charge carriers in the higher-lying energy states having a greater probability to be trapped.[52] However, due to the strong spectral overlap between $1P_h \rightarrow 1P_e$, $1S_h \rightarrow 1P_e$, and ESA bands, a precise determination of how much trapping versus relaxation (by comparing the relative magnitudes of the two signals) is extremely difficult.

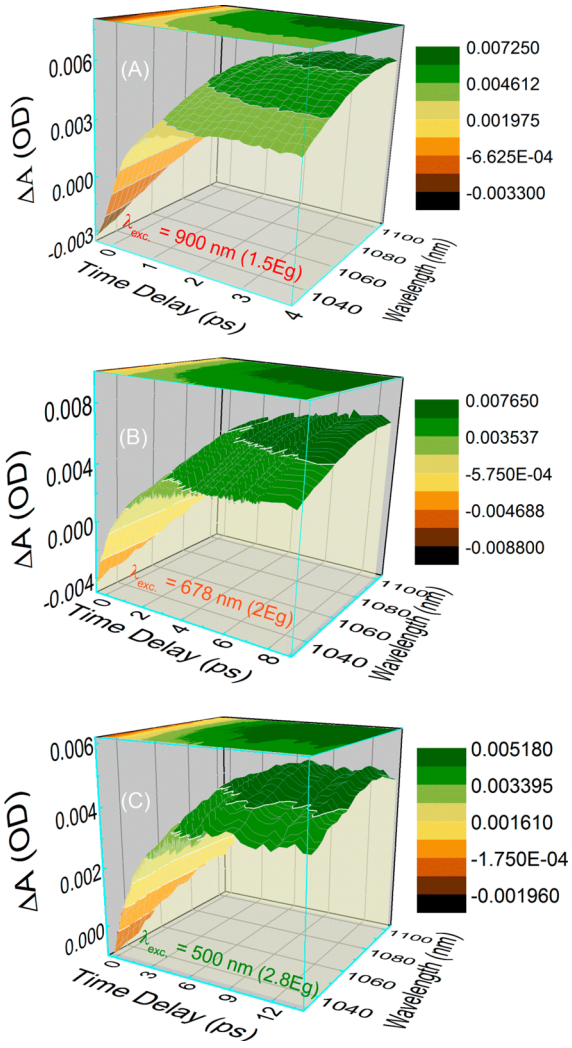


**Figure 3.** Three-dimensional surface and a corresponding contour plot of PbS-1355 with $E_g$ of 0.92 eV for pump-photon energy at wavelengths of 900 (A), 678 (B), and 500 nm (C), corresponding to 1.5, 2, and 2.8 times the $E_g$, respectively. The loading time of electrons from a higher state into the 1S state is very sensitive to the excitation photon energy.

Notably, as anticipated, the intraband relaxation becomes much faster as the QD size decreases. For instance, for the pump-photon energy at two times the $E_g$, the relaxation time is 2.6 ps for PbS-1560, and it shortens to 800 fs for PbS-1220. This demonstrates the key role of spatial confinement in the enhancement of the intraband relaxation as well as the absence of a phonon bottleneck. A similar size-dependent intraband relaxation has been observed in PbS and PbSe QDs with different $E_g$ values from 950 to 1950 nm.[42,53] The time constants of the intraband relaxation in PbS QDs in this study are comparable to an earlier report,[42] but they are longer than those in CdSe and PbSe QDs (on the order of 200 fs).[14,30,43] Interestingly, there is a linear relationship between the build-up time of the $1S_e$ state as a function of QD size and the pump-photon energy (Figure 5B,C). This would mean that the same initial excitonic states are not necessarily populated for each size of QD, because there are multiple channels by which a carrier


dx.doi.org/10.1021/ph500016t | ACS Photonics 2014, 1, 285−292

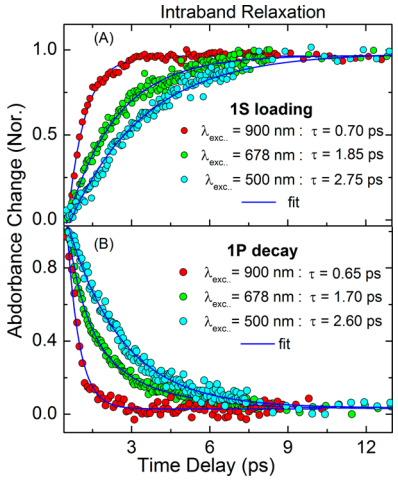


**Figure 4.** (A) ESA band of PbS-1355 at 1090 nm. The pump-photon energy as indicated in the figure. (B) The decay of the second exciton peak at 950 nm, which is associated with the $P_h \rightarrow P_e$ transition, indicating the direct 1P → 1S transition. The solid line represents the single exponential fit of the experimental data.

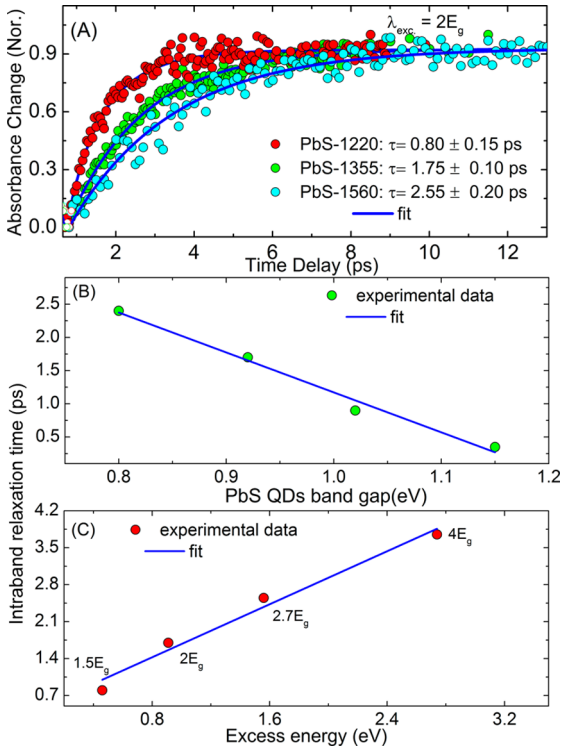


**Figure 5.** (A) 1P → 1S decay for different sizes of PbS QDs after photoexcitation at $2E_g$, showing that the intraband relaxation is very sensitive to the QD size, and the intraband relaxation time as a function of (B) $E_g$ and (C) the excess energy above the $E_g$.

can relax in semiconductor QDs. Each of these channels has a size dependence that is distinct.[54] However, to demonstrate this linear dependence quantitatively, we must turn to high-level theoretical investigations,[15] which are beyond the scope of this study.

The intraband transition in PbS QDs at high photon energies may be slowed down by the MEG process. However, because the dynamic responses of the ground state bleach and the ESA after the intraband relaxation are very similar and do not depend on the photon energy (see Supporting Information, SI), the possibility of a MEG process in PbS-1355 can also be ruled out under our chosen pump-photon excitation. Thus, a possible explanation for the slow intraband relaxation in PbS QDs is that the pump-photon energy at 1.5 or $2E_g$ can excite the QDs into the $1P_e$ or an admixture of $1S_e$ and $1P_e$ states with an exponential intraband $1P_e \rightarrow 1S_e$ transition taking place at a time constant of 0.65 and 1.80 ps, respectively, which is in contrast to an instantaneous population in the $1S_e$ state (see Figure 2A) when the pump-photon energy is at the first exciton absorption peak at 1355 nm ($1E_g$). At higher photon energies ($3E_g$ or $4E_g$), the excitation will be in a state higher in energy than 1P; thus, the initial electronic state could be a mixture of $1P_e$ and higher-lying states.[55] In this case, the average time constant of the relaxation process (2.80 and 3.40 ps, respectively) arises from the superposition of dynamics with different relaxation times, as the carrier relaxation will follow a sequential/hopping mechanism via subsequent lower-lying states with a complex kinetics profile, for example, $k_{2D\rightarrow 2P}$, $k_{2P\rightarrow 1P}$, $k_{1P\rightarrow 1S}$.[15,40] The overlap in time of these sequential processes gives rise to a single exponential profile with one time constant that is an average of the time constants of the stepwise processes. It should be noted that it is likely that a series of relaxation processes can give rise to single-exponential decay especially when the time constants of the dynamical events are not very well separated, as can be expected in our case, due to the high density of states. The observation of a single time constant out of sequential steps in other systems has been previously determined by time-resolved spectroscopy and supported by molecular dynamics simulations.[56] Given that the depopulation of the 1P state and the population of the 1S state is the dominant step, as indicated in Figure 4, the subpicosecond to few picosecond time constants of the intraband $1P_e \rightarrow 1S_e$ are in agreement with those reported by Van Stryland and co-workers.[42]

It is well documented by ultrafast time-resolved spectroscopic methodologies that there is a significant difference in the excited state population dynamics of single and multiple excitons.[2,4] More specifically, in the single exciton regime, the excited state dynamics are typically governed by a slow radiative decay corresponding to electron−hole recombination,[57] while in the presence of multiple excitons, an additional fast-decay component can be observed due to nonradiative Auger recombination, leaving only one exciton per individual QD.[2,11] In this sense, one can use this feature as a spectroscopic signature to track MEG processes in the time domain. Thus, to evaluate the MEG process in PbS QDs, in Figure 6, we present the TA data at different pump-photon energies for PbS QDs with band gaps of 1080 nm (1.15 eV). When we tuned the photon energy to 1 or 2 $E_g$ (for which MEG is not expected to occur), the ground state bleach showed a small decay on the picosecond time scale, and its amplitude was a few percent higher than the reported value for similarly sized PbS QDs.[58] This decay may be attributed to state trapping (which lies just below the first confined electron state)[52] due to the uncapped QD surface, which provides additional recombination pathways.[45] In this regard, we note that, although individual organic ligands can efficiently passivate surface trap states, the steric hindrance between adjacent ligands makes complete surface coverage unrealistic.[59] More importantly, it has been emphasized that carrier multiplication occurs more rapidly than does the capture of excited carriers in traps.[52] As a result, this small decay and its dynamics may not add appreciable uncertainty to the estimation of MEG. On the other hand, we


dx.doi.org/10.1021/ph500016t | ACS Photonics 2014, 1, 285−292

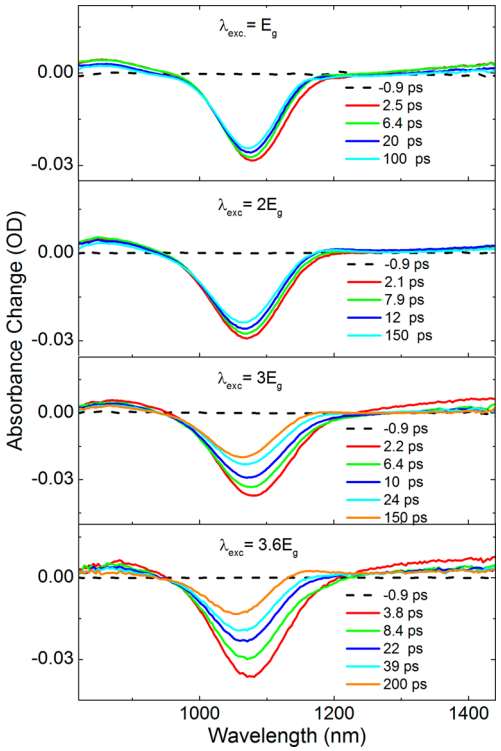


**Figure 6.** Series of TA spectra for PbS-1080 for pump-photon energies of 1, 2, 3, and 3.7 $E_g$. For pump excitations higher than $2E_g$, there is an additional fast component that corresponds to the multiple-exciton generation. On the other hand, no measurable MEG is observed for excitation at $2E_g$, in good agreement with recent TA data reported on a similar QD size.[29]

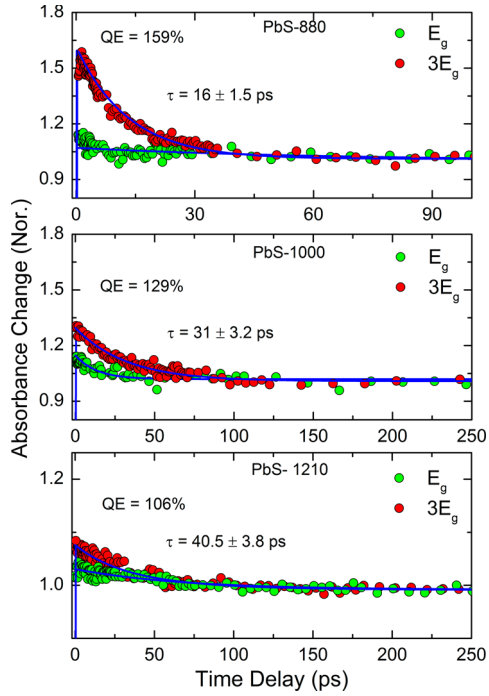


**Figure 7.** Bleach of the first exciton state for PbS-880 and PbS-1000 at photon energies of $1E_g$ (green) and $3E_g$ (red). By dividing the initial TA signal amplitude (multiexciton) by the long-time signal (single exciton), photoexcitation quantum efficiencies of PbS QDs were calculated. Note that the sign of the signal is reversed and normalized for clarity.

emphasize that increasing the pump-photon energy well above the quantum-confined band gap causes a clear acceleration of the bleach decay and increases the percentage of its recovery due to Auger recombination processes of multiple electron−hole pairs (Figure 6C,D), providing clear evidence of the increasing number of electron−hole pairs with increased pump-photon energy. It should be noted that with the pump excitation fluences in our experiments, the average number of photons absorbed per QD per pump pulse was about 0.18. Under this condition, one exciton per dot is assured, and thus the estimation of MEG is valid,[60] but for accuracy of MEG estimation,[60] based on Poisson distribution of photon absorption events, the direct generation of multiple excitons via absorption of multiple photons has been corrected. Moreover, we should also emphasize that the transition to the MEG regime results not only in the change in population dynamics (due to activation of Auger decay) but it also dramatically modifies the spectral response of the quantum dots.

Figure 7 shows a comparison of the bleach recovery dynamics, on the hundreds of picoseconds time scale, for different sizes of PbS QDs at a photon energy equal to $1E_g$ (for which no MEG is expected) and $3E_g$. A global fitting procedure for the bleach recovery of PbS-880, PbS-1000, and PbS-1210 indicated that the additional fast component due to non-radiative Auger recombination is significantly faster when going from bigger to smaller QD sizes. For instance, the recombination time is 40 ps for PbS-1210, and it shortens to 31 and 16 ps for PbS-1000 and PbS-880, respectively. It is clear that the recombination time correlates linearly with the estimated volume of PbS-1210, PbS-1000, and PbS-880 (39, 33, and 18 $nm^3$, respectively). Such a linear correlation between Auger lifetimes with QD volume has been pointed out for CdSe, PbSe, and PbS QDs.[39,61]

Since the magnitude of the ground state bleach recovery is directly proportional to the exciton depopulation, it is possible to determine the average number of electron−hole pairs ($N_x$) generated by a single high-energy photon. The $N_x$ is calculated as the ratio between the initial signal amplitude (multiexciton) and the long-time signal amplitude (single exciton). MEG QY can be estimated as QY = $100N_x$, and the biexciton yield of photon-to-exciton conversion is calculated from $\eta_{xx}$ = QY-100. It is worth mentioning that the solution was constantly stirred to have a fresh sample volume for each laser shot to exclude any signal contribution from photocharging (see Experimental Section in the SI). As can be seen in Figure 7A,B, a MEG QY of 159 and 129% can be achieved for PbS-880 and PbS-1000, respectively, at the pump-photon excitation of $3E_g$. Note that the pump fluence at $3E_g$ especially for Pb-880 is too low to keep the average absorbed photon at 0.18. Based on repeated experiments, the sensitivity of the power meter, and the beam-size measurements, the error bar was estimated to be about 10%. We also determined that, at $3E_g$, the MEG of PbS-1210 is 106%, which is fairly in agreement with a value reported recently (112%) for a similar PbS QD size.[62] On the other hand, under the same experimental conditions, we found $N_x \approx 1$ for PbS-1355 and PbS-1560 (see SI), indicating the absence of MEG. This finding is also in good agreement with recent TA data reported on a similar QD size.[29] More specifically, for PbS-1560, the exciton multiplication energy threshold is higher than $4E_g$ (data not shown), and it may tend to match that of bulk PbS.[42] In this regime, the QY of multiple-exciton generation at


dx.doi.org/10.1021/ph500016t | ACS Photonics 2014, 1, 285−292

a pump-photon energy of $3E_g$ as a function of the QD band gap is presented in Figure 8. The higher MEG QY with the

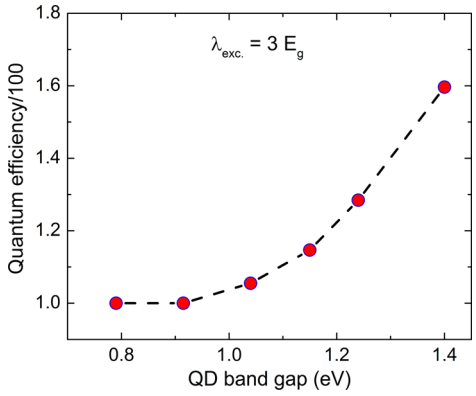


**Figure 8.** QY of multiple-exciton generation at a pump−photon energy of $3E_g$ as a function of the QD's band gap, demonstrating that the efficiency of the carrier-multiplication increases with decreasing QD size.

decrease in PbS QD size demonstrates that the efficiency of the carrier-multiplication increases with decreasing QD size. This finding underscores the important notion in recent reports that MEG QY of this type of QD is strongly size-dependent, whereas the MEG QY of PbSe QDs is size-independent.[61,63] It also further demonstrates the critical role of the confinement on the dynamics of Auger recombination of multiple electron−hole pairs in PbS QDs. The distinct size-dependent trends in MEG QY in PbS and PbSe QDs has been attributed to the differing behaviors of the energy-loss rate related to non-MEG processes.[61] This means that, in smaller PbS QDs, the strong confinement induces enhancement in the Coulomb interactions due to closer proximity of the charge carriers, reducing the energy required to generate a new electron−hole pair after the MEG threshold is achieved.[61] In the regime of multiple e−h pairs, the extracted kinetics indicates that the carrier dynamics becomes faster as the number of e−h pairs increases. This is not surprising, because multiple e−h pairs lead to an increase in the Auger-accelerated multiple-exciton recombination.[14,60,63]

## CONCLUSIONS

Using femtosecond broadband transient absorption spectroscopy, we presented the carrier state-to-state intraband relaxation in colloidal PbS QDs and resolved the carrier loading time into the band edge from an arbitrary initial state prepared by photoexcitation above the effective band gap. We found that the 1P → 1S carrier relaxation time is ultrafast (sub- to picosecond time scales), and it depends strongly on the initial state, which is related to the pump-photon energy. Moreover, our results indicate that the intraband relaxation of PbS QDs is very sensitive to QD size; it becomes much faster as the size of the QDs decreases, demonstrating the key role of high carrier density in smaller QDs in intraband relaxation dynamics. The data unambiguously demonstrate that the carrier intraband relaxation in PbS QDs is sufficiently fast to be completed successfully before nonradiative Auger recombination becomes competitive. Our findings on the state-to-state transition might be an important adjustable parameter in future theoretical studies that analyze precisely the MEG mechanism. In addition to the state-to-state relaxation dynamics, we report a quantitative analysis of MEG as a function of QD size, which can be identified via electronic spectroscopy on the basis of the fast decay of the Auger recombination. At a photon excitation above the energy threshold of MEG, fast exciton Auger recombination dynamics is evident, serving as a spectroscopic signature for MEG. Quantitative analysis of the data reveals that MEG is a function of QD size, where large-sized QDs exhibit a higher MEG threshold and, subsequently, lower QY compared with the small-sized QDs. As a consequence, the threshold photon energy for MEG in QDs, which is reported to be twice the lowest exciton absorption energy (the limit defined by energy conservation), cannot be generalized for all QD sizes. Thus, MEG estimation is expected to depend not only on pump-photon energy but also on the particle size.

## METHODS

**PbS QDs Preparation.** Oleic-acid capped PbS quantum dots were synthesized using lead oleate and bis(trimethylsilyl) sulfide as precursors in 1-octadecene, as described elsewhere[64] (also see the SI for details). The steady-state absorption spectra of the PbS QDs dispersed in toluene were measured using a Cary 5000 UV−vis-NIR spectrophotometer (Varian Inc.). Note that we refer to our QD samples based on the wavelength of their LUMO−HOMO transition energy. For instance, we call the sample with a $1S_h-1S_e$ peak at 1355 nm, which is related to the energy band gap ($E_g$) in the semiconductor and equivalent to the LUMO−HOMO transition energy in molecular systems, as PbS-1355.

**Transmission Electron Microscopy (TEM).** TEM images were obtained using a TitanG2 80−300 instrument equipped with an image-corrector from CEOS and an energy-filter (Gatan Inc.) was used for the high-resolution TEM (HRTEM) characterization of the QDs. The PbS QDs sample was obtained by deposition of the QDs suspended in a toluene solution on an ultrathin carbon film on 400-mesh copper grids, followed by drying in air for at least 1 h before imaging.

**Pump−Probe Transient Absorption (TA) Spectroscopy.** In the pump−probe transient absorption experiments, a white light continuum probe pulse was generated in a 2 mm-thick sapphire plate contained in an Ultrafast System LLC spectrometer by a few $\mu$J pulse energy of the fundamental output of a Ti:Sapphire femtosecond regenerative amplifier operating at 800 nm with 35 fs pulses and a repetition rate of 1 kHz. The spectrally tunable (240−2600 nm) femtosecond pulses generated in the Optical Parametric Amplifier (Newport Spectra-Physics) and the white light continuum were used as a pump (excitation)- and probe-beam in the pump−probe experimental setup (Helios; see SI for details).

The optical density of all PbS QDs colloidal solutions in a 2 mm path length cuvette was adjusted to approximately 0.1 at the $1S_h-1S_e$ transition peak. The solution was constantly stirred using a magnetic stirrer to have a fresh sample for each laser shot to avoid photocharging of the QDs, which leads to a solid deposition on the walls of the spectroscopic quartz cells.[65] To check for possible nonlinear effects induced by multiphoton absorption, the time-resolved experiments were performed at low pump fluence. In this regard, to explore MEG resulting only from single-photon absorption, we maintained the average number of photons ($N_{ph}$) absorbed per QD per pump pulse at the entrance face of our TA setup to be less than 0.2, ensuring that the photoexcited QDs are due to single-photon absorption.[26] We found that the UV−vis absorption spectrum of each sample measured before and after every pump−probe


dx.doi.org/10.1021/ph500016t | ACS Photonics 2014, 1, 285−292

experiment did not show any degradation. All TA experiments were carried out at room temperature.

## ■ ASSOCIATED CONTENT

### Supporting Information

Descriptions of PbS QDs synthesis and preparation as well as experimental setup of the transient absorption spectroscopy. This material is available free of charge via the Internet at http://pubs.acs.org.

## ■ AUTHOR INFORMATION


### Corresponding Author

*E-mail: omar.abdelsaboor@kaust.edu.sa; osman.bakr@kaust.edu.sa.

### Author Contributions

†These authors contributed equally to the work (A.O.E.-B. and E.A.).


### Notes

The authors declare no competing financial interest.

## ■ REFERENCES


(1) Schaller, R. D.; Klimov, V. I. High efficiency carrier multiplication in PbSe nanocrystals: Implications for solar energy conversion. *Phys. Rev. Lett.* **2004**, *92*, 186601.

(2) McGuire, J. A.; Joo, J.; Pietryga, J. M.; Schaller, R. D.; Klimov, V. I. New aspects of carrier multiplication in semiconductor nanocrystals. *Acc. Chem. Res.* **2008**, *41*, 1810−1819.

(3) Ji, M.; Park, S.; Connor, S. T.; Mokari, T.; Cui, Y.; Gaffney, K. J. Efficient multiple exciton generation observed in colloidal PbSe quantum dots with temporally and spectrally resolved intraband excitation. *Nano Lett.* **2009**, *9*, 12171−1222.

(4) Wang, S.; Khafizov, M.; Tu, X.; Zheng, M.; Krauss, T. D. Multiple exciton generation in single-walled carbon nanotubes. *Nano Lett.* **2010**, *10*, 2381−2386.

(5) Baer, R.; Rabani, E. Can impact excitation explain efficient carrier multiplication in carbon nanotube photodiodes? *Nano Lett.* **2010**, *10*, 3277−3282.

(6) Lohse, S. E.; Murphy, C. J. Applications of colloidal inorganic nanoparticles: From medicine to energy. *J. Am. Chem. Soc.* **2012**, *134*, 15607−15620.

(7) Li, L.; Yang, X.; Gao, J.; Tian, H.; Zhao, J.; Hagfeldt, A.; Sun, L. Highly efficient CdS quantum dot-sensitized solar cells based on a modified polysulfide electrolyte. *J. Am. Chem. Soc.* **2011**, *133*, 8458−8460.

(8) Santra, P. K.; Kamat, P. V. Mn-doped quantum dot sensitized solar cells: A strategy to boost efficiency over 5%. *J. Am. Chem. Soc.* **2012**, *134*, 2508−2511.

(9) Pijpers, J. J. H.; Ulbricht, R.; Tielrooij, K. J.; Osherov, A.; Golan, Y.; Delerue, C.; Allan, G.; Bonn, M. Assessment of carrier-multiplication efficiency in bulk PbSe and PbS. *Nat. Phys.* **2009**, *5*, 811−814.

(10) Kambhampati, P. Unraveling the structure and dynamics of excitons in semiconductor quantum dots. *Acc. Chem. Res.* **2011**, *44*, 1−13.

(11) Beard, M. C.; Luther, J. M.; Semonin, O. E.; Schaller, R. D.; Nozik, A. J. Third generation photovoltaics based on multiple exciton generation in quantum confined semiconductors. *Acc. Chem. Res.* **2012**, *46*, 1252−1260.

(12) Hsu, S.-H.; Hung, S.-F.; Chien, S.-H. CdS sensitized vertically aligned single crystal $TiO_2$ nanorods on transparent conducting glass with improved solar cell efficiency and stability using ZnS passivation layer. *J. Power Sources* **2013**, *233*, 236−243.

(13) Shockley, W.; Queisser, H. J. Detailed balance limit of efficiency of *p*−*n* junction solar cells. *J. Appl. Phys.* **1961**, *32*, 510−519.

(14) Ellingson, R. J.; Beard, M. C.; Johnson, J. C.; Yu, P. R.; Micic, O. I.; Nozik, A. J.; Shabaev, A.; Efros, A. L. Highly efficient multiple exciton generation in colloidal PbSe and PbS quantum dots. *Nano Lett.* **2005**, *5*, 865−871.

(15) Shabaev, A.; Efros, A. L.; Nozik, A. J. Multiexciton generation by a single photon in nanocrystals. *Nano Lett.* **2006**, *6*, 2856−2863.

(16) Nozik, A. J. Multiple exciton generation in semiconductor quantum dots. *Chem. Phys. Lett.* **2008**, *457*, 3−11.

(17) Allan, G.; Delerue, C. Role of impact ionization in multiple exciton generation in PbSe nanocrystals. *Phys. Rev. B* **2006**, *73*, 205423.

(18) Luther, J. M.; Beard, M. C.; Song, Q.; Law, M.; Ellingson, R. J.; Nozik, A. J. Multiple exciton generation in films of electronically coupled PbSe quantum dots. *Nano Lett.* **2007**, *7*, 1779−1784.

(19) Schaller, R. D.; Pietryga, J. M.; Klimov, V. I. Carrier multiplication in InAs nanocrystal quantum dots with an onset defined by the energy conservation limit. *Nano Lett.* **2007**, *7*, 3469−3476.

(20) Beard, M. C.; Knutsen, K. P.; Yu, P.; Luther, J. M.; Song, Q.; Metzger, W. K.; Ellingson, R. J.; Nozik, A. J. Multiple exciton generation in colloidal silicon nanocrystals. *Nano Lett.* **2007**, *7*, 2506−2512.

(21) Pijpers, J. J. H.; Hendry, E.; Milder, M. T. W.; Fanciulli, R.; Savolainen, J.; Herek, J. L.; Vanmaekelbergh, D.; Ruhman, S.; Mocatta, D.; Oron, D.; et al. Carrier multiplication and its reduction by photodoping in colloidal InAs quantum dots. *J. Phys. Chem. C* **2007**, *111*, 4146−4152.

(22) Schaller, R. D.; Sykora, M.; Pietryga, J. M.; Klimov, V. I. Seven excitons at a cost of one: Redefining the limits for conversion efficiency of photons into charge carriers. *Nano Lett.* **2006**, *6*, 424−429.

(23) Ben-Lulu, M.; Mocatta, D.; Bonn, M.; Banin, U.; Ruhman, S. On the absence of detectable carrier multiplication in a transient absorption study of InAs/CdSe/ZnSe core/shell1/shell2 quantum dots. *Nano Lett.* **2008**, *8*, 1207−1211.

(24) Nair, G.; Geyer, S. M.; Chang, L. Y.; Bawendi, M. G. Carrier multiplication yields in PbS and PbSe nanocrystals measured by transient photoluminescence. *Phys. Rev. B* **2008**, *78*, 125325.

(25) Nair, G.; Bawendi, M. G. Carrier multiplication yields of CdSe and CdTe nanocrystals by transient photoluminescence spectroscopy. *Phys. Rev. B* **2007**, *76*, 081304.

(26) McGuire, J. A.; Sykora, M.; Joo, J.; Pietryga, J. M.; Klimov, V. I. Apparent versus true carrier multiplication yields in semiconductor nanocrystals. *Nano Lett.* **2010**, *10*, 2049−2057.

(27) Norris, D. J.; Bawendi, M. G. Measurement and assignment of the size-dependent optical spectrum in CdSe quantum dots. *Phys. Rev. B* **1996**, *53*, 16338−16346.

(28) Alivisatos, A. P. Perspectives on the physical chemistry of semiconductor nanocrystals. *J. Phys. Chem.* **1996**, *100*, 13226−13239.

(29) Gesuele, F.; Sfeir, M. Y.; Koh, W. K.; Murray, C. B.; Heinz, T. F.; Wong, C. W. Ultrafast supercontinuum spectroscopy of carrier multiplication and biexcitonic effects in excited states of PbS quantum dots. *Nano Lett.* **2012**, *12*, 2658−2664.

(30) Klimov, V. I. Optical nonlinearities and ultrafast carrier dynamics in semiconductor nanocrystals. *J. Phys. Chem. B* **2000**, *104*, 6112−6123.

(31) Klimov, V. I.; Karavanskii, V. A. Mechanisms for optical nonlinearities and ultrafast carrier dynamics in $Cu_xS$ nanocrystals. *Phys. Rev. B* **1996**, *54*, 8087−8094.

(32) Woggon, U.; Giessen, H.; Gindele, F.; Wind, O.; Fluegel, B.; Peyghambarian, N. Ultrafast energy relaxation in quantum dots. *Phys. Rev. B* **1996**, *54*, 17681−17690.

(33) Klimov, V. I.; HaringBolivar, P.; Kurz, H.; Karavanskii, V. A. Optical nonlinearities and carrier trapping dynamics in CdS and $Cu_xS$ nanocrystals. *Superlattices Microstruct.* **1996**, *20*, 395−404.

(34) Burda, C.; Link, S.; Mohamed, M.; El-Sayed, M. The relaxation pathways of CdSe nanoparticles monitored with femtosecond time-resolution from the visible to the IR: Assignment of the transient features by carrier quenching. *J. Phys. Chem. B* **2001**, *105*, 12286−12292.

(35) Landes, C.; Burda, C.; Braun, M.; El-Sayed, M. A. Photoluminescence of CdSe nanoparticles in the presence of a hole acceptor: *n*-Butylamine. *J. Phys. Chem. B* **2001**, *105*, 2981−2986.
(36) Mohamed, M. B.; Burda, C.; El-Sayed, M. A. Shape dependent ultrafast relaxation dynamics of CdSe nanocrystals: Nanorods vs nanodots. *Nano Lett.* **2001**, *1*, 589−593.
(37) Klimov, V. I.; McBranch, D. W. Femtosecond 1P-to-1S electron relaxation in strongly confined semiconductor nanocrystals. *Phys. Rev. Lett.* **1998**, *80*, 4028−4031.
(38) Klimov, V. I.; Mikhailovsky, A. A.; McBranch, D. W.; Leatherdale, C. A.; Bawendi, M. G. Mechanisms for intraband energy relaxation in semiconductor quantum dots: The role of electron−hole interactions. *Phys. Rev. B* **2000**, *61*, 13349−13352.
(39) Klimov, V. I.; Mikhailovsky, A. A.; Xu, S.; Malko, A.; Hollingsworth, J. A.; Leatherdale, C. A.; Eisler, H. J.; Bawendi, M. G. Optical gain and stimulated emission in nanocrystal quantum dots. *Science* **2000**, *290*, 314−317.
(40) Sewall, S. L.; Cooney, R. R.; Dias, E. A.; Tyagi, P.; Kambhampati, P. State-resolved observation in real time of the structural dynamics of multiexcitons in semiconductor nanocrystals. *Phys. Rev. B* **2011**, *84*, 235304.
(41) Klimov, V. I.; Mikhailovsky, A. A.; McBranch, D. W.; Leatherdale, C. A.; Bawendi, M. G. Quantization of multiparticle Auger rates in semiconductor quantum dots. *Science* **2000**, *287*, 1011−1013.
(42) Nootz, G.; Padilha, L. A.; Levina, L.; Sukhovatkin, V.; Webster, S.; Brzozowski, L.; Sargent, E. H.; Hagan, D. J.; Stryland, E. W. V. Size dependence of carrier dynamics and carrier multiplication in PbS quantum dots. *Phys. Rev. B* **2011**, *83*, 155302.
(43) Kambhampati, P. Hot exciton relaxation dynamics in semiconductor quantum dots: Radiationless transitions on the nanoscale. *J. Phys. Chem. C* **2011**, *115*, 22089−22109.
(44) Ouyang, J.; Schuurmans, C.; Zhang, Y.; Nagelkerke, R.; Wu, X.; Kingston, D.; Wang, Z. Y.; Wilkinson, D.; Li, C.; Leek, D. M.; et al. Low-temperature approach to high-yield and reproducible syntheses of high-quality small-sized PbSe colloidal nanocrystals for photovoltaic applications. *ACS Appl. Mater. Interfaces* **2011**, *3*, 553−565.
(45) Fitzmorris, B. C.; Pu, Y.-C.; Cooper, J. K.; Lin, Y.-F.; Hsu, Y.-J.; Li, Y.; Zhang, J. Z. Optical properties and exciton dynamics of alloyed core/shell/shell $Cd_{1-x}Zn_xSe$/ZnSe/ZnS quantum dots. *ACS Appl. Mater. Interfaces* **2013**, *5*, 2893−2900.
(46) Nandwana, V.; Serrano, L. A.; Solntsev, K. M.; Ebenhoch, B.; Liu, Q.; Tonga, G. Y.; Samuel, I. D. W.; Cooke, G.; Rotello, V. M. Engineering the nanoscale morphology of a quantum dot−fullerene assembly via complementary hydrogen bonding interactions. *Langmuir* **2013**, *29*, 7534−7537.
(47) Pelton, M.; Ithurria, S.; Schaller, R. D.; Dolzhnikov, D. S.; Talapin, D. V. Carrier cooling in colloidal quantum wells. *Nano Lett.* **2012**, *12*, 6158−6163.
(48) Santori, C.; Solomon, G. S.; Pelton, M.; Yamamoto, Y. Time-resolved spectroscopy of multiexcitonic decay in an InAs quantum dot. *Phys. Rev. B* **2002**, *65*, 073310.
(49) Klimov, V. I.; Hunsche, S.; Kurz, H. Biexciton effects in femtosecond nonlinear transmission of semiconductor quantum dots. *Phys. Rev. B* **1994**, *50*, 8110−8113.
(50) Miller, D. A. B.; Chemla, D. S.; Damen, T. C.; Gossard, A. C.; Wiegmann, W.; Wood, T. H.; Burrus, C. A. Band-edge electroabsorption in quantum well structures: The quantum-confined Stark effect. *Phys. Rev. Lett.* **1984**, *53*, 2173−2176.
(51) Klimov, V. I.; McBranch, D. W.; Leatherdale, C. A.; Bawendi, M. G. Electron and hole relaxation pathways in semiconductor quantum dots. *Phys. Rev. B* **1999**, *60*, 13740−13749.
(52) Sukhovatkin, V.; Hinds, S.; Brzozowski, L.; Sargent, E. H. Colloidal quantum-dot photodetectors exploiting multiexciton generation. *Science* **2009**, *324*, 1542−1544.
(53) Schaller, R. D.; Pietryga, J. M.; Goupalov, S. V.; Petruska, M. A.; Ivanov, S. A.; Klimov, V. I. Breaking the phonon bottleneck in semiconductor nanocrystals via multiphonon emission induced by intrinsic nonadiabatic interactions. *Phys. Rev. Lett.* **2005**, *95*, 169401.
(54) Cooney, R. R.; Sewall, S. L.; Dias, E. A.; Sagar, D. M.; Anderson, K. E. H.; Kambhampati, P. Unified picture of electron and hole relaxation pathways in semiconductor quantum dots. *Phys. Rev. B* **2007**, *75*, 245311.
(55) Wang, L. W.; Zunger, A. High-energy excitonic transitions in CdSe quantum dots. *J. Phys. Chem. B* **1998**, *102*, 6449−6454.
(56) Lin, M. M.; Mohammed, O. F.; Jas, G. S.; Zewail, A. H. Speed limit of protein folding evidenced in secondary structure dynamics. *Proc. Natl. Acad. Sci. U.S.A.* **2011**, *108*, 16622−16627.
(57) Wehrenberg, B. L.; Wang, C. J.; Guyot-Sionnest, P. Interband and intraband optical studies of PbSe colloidal quantum dots. *J. Phys. Chem. B* **2002**, *106*, 10634−10640.
(58) Yang, Y.; Rodriguez-Cordoba, W.; Lian, T. Ultrafast charge separation and recombination dynamics in lead sulfide quantum dot-methylene blue complexes probed by electron and hole intraband transitions. *J. Am. Chem. Soc.* **2011**, *133*, 9246−9249.
(59) Lees, E. E.; Gunzburg, M. J.; Nguyen, T.-L.; Howlett, G. J.; Rothacker, J.; Nice, E. C.; Clayton, A. H. A.; Mulvaney, P. Experimental determination of quantum dot size distributions, ligand packing densities, and bioconjugation using analytical ultracentrifugation. *Nano Lett.* **2008**, *8*, 2883−2890.
(60) Istrate, E.; Hoogland, S.; Sukhovatkin, V.; Levina, L.; Myrskog, S.; Smith, P. W. E.; Sargent, E. H. Carrier relaxation dynamics in lead sulfide colloidal quantum dots. *J. Phys. Chem. B* **2008**, *112*, 2757−2760.
(61) Stewart, J. T.; Padilha, L. A.; Qazilbash, M. M.; Pietryga, J. M.; Midgett, A. G.; Luther, J. M.; Beard, M. C.; Nozik, A. J.; Klimov, V. I. Comparison of carrier multiplication yields in PbS and PbSe nanocrystals: The role of competing energy-loss processes. *Nano Lett.* **2012**, *12*, 622−628.
(62) Yang, Y.; Rodriguez-Cordoba, W.; Lian, T. Multiple exciton generation and dissociation in PbS quantum dot-electron acceptor complexes. *Nano Lett.* **2012**, *12*, 4235−4241.
(63) Midgett, A. G.; Luther, J. M.; Stewart, J. T.; Smith, D. K.; Padilha, L. A.; Klimov, V. I.; Nozik, A. J.; Beard, M. C. Size and composition dependent multiple exciton generation efficiency in PbS, PbSe, and $PbS_xSe_{1-x}$ alloyed quantum dots. *Nano Lett.* **2013**, *13*, 3078−3085.
(64) Hines, M. A.; Scholes, G. D. Colloidal PbS nanocrystals with size-tunable near-infrared emission: Observation of post-synthesis self-narrowing of the particle size distribution. *Adv. Mater.* **2003**, *15*, 1844−1849.
(65) Hardman, S. J. O.; Graham, D. M.; Stubbs, S. K.; Spencer, B. F.; Seddon, E. A.; Fung, H.-T.; Gardonio, S.; Sirotti, F.; Silly, M. G.; Akhtar, J.; et al. Electronic and surface properties of PbS nanoparticles exhibiting efficient multiple exciton generation. *Phys. Chem. Chem. Phys.* **2011**, *13*, 20275−202083.